COMPDYN 2011
3rd ECCOMAS Thematic Conference on
Computational Methods in Structural Dynamics and Earthquake Engineering
M. Papadrakakis, M. Fragiadakis, V. Plevris (eds.)
Corfu, Greece, 25–28 May 2011

A STUDY OF THE INFLUENCE OF THE RIGIDITY OF JOINTS ON THE DYNAMIC RESPONSE OF STEEL STRUCTURES

A.A. Vrakas[1] & M. Papadrakakis[2]

[1, 2] Institute of Structural Analysis and Antiseismic Research
National Technical University of Athens
Zografou Campus, Athens 15780, Greece
avrakas@central.ntua.gr, mpapadra@central.ntua.gr

Keywords: beam-to-column joints, rigidity of joints, steel frames, detailed finite element modeling, *M-φ* curves, direct-integration nonlinear dynamic analysis, seismic response

Abstract. *The objective of this paper is to study the influence of the rigidity of joints on the nonlinear dynamic response of steel structures under seismic excitation. We consider bolted beam-to-column joints with extended end-plates. A detailed finite element simulation of the joints is performed using structural (beam and shell) and three-dimensional continuum (eight-node hexahedral solid) elements. Material as well as geometric nonlinearities with contact between the appropriate components of the connections are taken into account. The moment-rotation (M-φ) response of characteristic joints, subjected to static loads, is calculated and compared with experimental results and EC3 predictions for the validation of the corresponding numerical models. The dynamic response of steel frames is examined, with detailed modeling of their joints via structural elements according to the above study, capturing all types of nonlinearities. Frame members are modeled either with shell (full simulation) or with beam elements combined with proper compatibility constraints at the interfaces with the joints (hybrid simulation) accounting for the excessive computational effort required to perform nonlinear dynamic analyses with detailed finite element models. Implicit direct-integration is implemented in order to study the nonlinear seismic response of the above frame models, while El Centro earthquake horizontal accelerogram is considered for the seismic excitation. In order to study the influence of the joints end-plate and bolts, parametric analyses are performed demonstrating the effect of each component on the overall dynamic behavior of steel structures. Time history curves of nodal displacements are displayed for the appropriate comparisons. The detailed finite element discretization of the joint and frame models is produced automatically from the corresponding geometric models.*

1 INTRODUCTION

Bolted beam-to-column joints with extended end-plates are used widely in steel structures. They form moment-resistant connections between steel members, but their behavior can be either rigid or semi-rigid depending on the stiffness and strength of their components. The consideration of semi-rigid connections corresponds to a more realistic simulation of the joints behavior leading to more reliable solutions. However, the large number of variables related to connection geometry makes the task of incorporating semi-rigid behavior of the connections into the frame design a complicated process. Additionally, structural joints may exhibit nonlinear behavior such as localized elastoplastic deformations, unilateral contact and slip phenomena. The behavior of steel joints has been the subject of both experimental [12-17] and numerical [5-11] studies by a number of researchers.

This paper first presents a finite element study of semi-rigid joints subjected to static loading. Stiffness, moment resistance and rotation capacity derived from the calculation of moment-rotation (M-φ) curves are compared with experimental results by Coelho et al. [12] and Eurocode 3 suggestions [2]. Then, multi-storey steel frames with detailed modeling of their connections according to the above study are subjected to seismic excitation in order to examine the influence of the rigidity of joints on the dynamic response of moment-resistant steel structures [16-17]. Parametric studies are performed demonstrating how variations of geometric characteristics of joint components can change the connection behavior and consequently the seismic response of steel frames. Moreover, various finite element simulations are investigated in order to find hybrid models of detailed finite element simulation of joints combined with beam simulation for the structural elements in an effort to combine accuracy and low computational cost. The finite element discretization of joints and structural elements is produced automatically from their geometric description. ABAQUS/Standard software is used for the static and dynamic numerical analyses of this paper [1].

2 FINITE ELEMENT MODELING OF STEEL JOINTS

2.1 Simulation with shell elements

Two different element types are used for modeling the end-plate bolted beam-to-column joint (Fig. 1). Plane components of the joint (beam/column flanges and web, end-plate, transverse web stiffeners) are modeled with the S4 quadrilateral shell element of appropriate thickness, while the bolts are modeled with beam elements of circular section. The interaction between the column flange and the end-plate is considered through surface-based contact simulation with element-based surface definition, which enables contact between independent meshes without node compatibility.

2.2 Simulation with continuum elements

Three-dimensional eight-node hexahedral solid elements are used for the detailed simulation of the extended end-plate bolted beam-to-column joint (Figs. 2, 3). Apart from the finite element discretization difficulties using three-dimensional solid elements, there are many complexities related to the contacts between the different components of a beam-to-column bolted joint. Particularly, there are five interactions that should be considered: (a) column flange with end-plate; (b) column flange with bolt head; (c) end-plate with bolt nut; (d) column flange hole with bolt shank; and (e) end-plate hole with bolt shank. All of them are modeled by using surface-based contacts with element-based surface definition that enables connection of independent meshes. Surfaces are defined through the appropriate faces of the hexahedral solids. More specifically, for cases (a), (d) and (e) small sliding contact formulation is considered

with a softened contact relationship. The slope of the linear pressure-overclosure curve is taken equal to 10^5. The tangential behavior of the interfaces is modeled through the basic isotropic Coulomb friction model with a constant coefficient μ equal to 0.30. For the other cases tied contact simulation is considered, where each node on the slave surface has the same displacement with the corresponding contact point on the master surface.

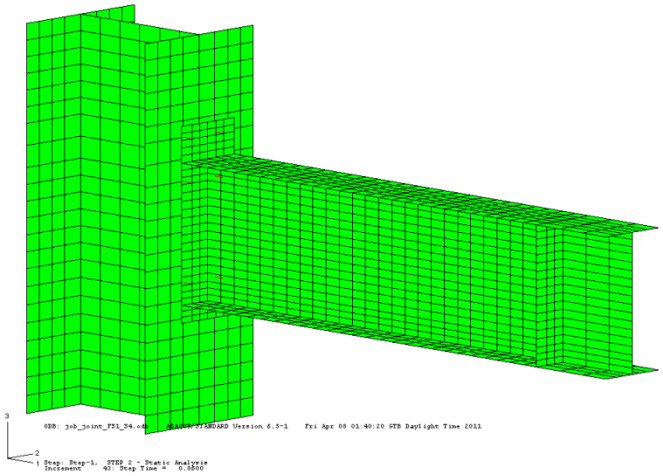

Figure 1: Joint simulation with shell (quadrilateral) finite elements

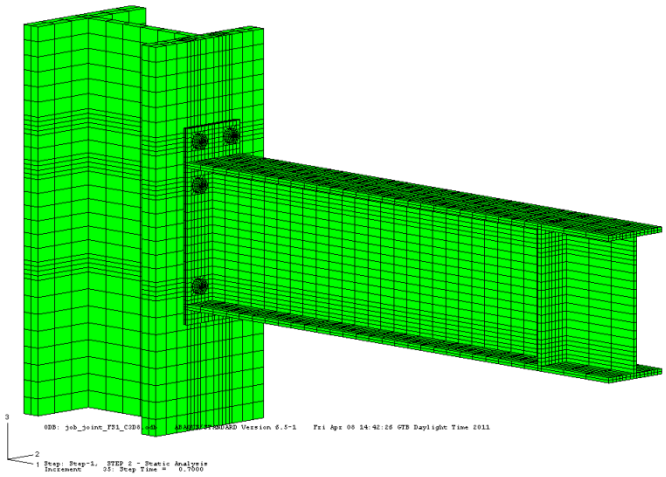

Figure 2: Joint simulation with continuum (8-node hexahedral solid) finite elements

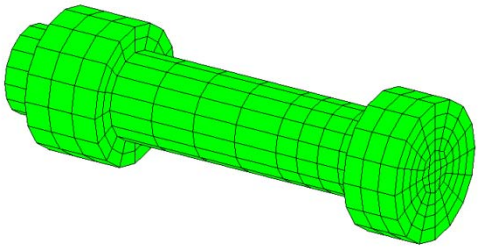

Figure 3: Bolt simulation with continuum (8-node hexahedral solid) finite elements

2.3 Experimental data

An experimental investigation of eight statically loaded extended end-plate moment connections was undertaken at the Delft University of Technology by Coelho et al. [12] to provide insight into the behavior of this type of joint up to collapse. The specimens were designed to confine failure to the end-plate and/or bolts without development of the full plastic moment capacity of the beam. The parameters investigated were the end-plate thickness and steel grade. Details of the test specimens are given in Table 1.

Test ID	Number	Column		Beam		End-plate	
		Profile	Steel grade	Profile	Steel grade	t_p (mm)	Steel grade
FS1	2	HEM340	S355	IPE300	S235	10	S355
FS2	2	HEM340	S355	IPE300	S235	15	S355
FS3	2	HEM340	S355	IPE300	S235	20	S355
FS4	2	HEM340	S355	IPE300	S235	10	S690

Table 1: Details of the test specimens [12]

2.4 Numerical results

The detailed geometry of the connections is considered in the numerical analyses performed. Hand tightened full-threaded M20 grade 8.8 bolts were used, which are modeled via an equivalent diameter of 18.80 mm that derives from the average of the gross diameter 20.00 mm and the effective diameter of the bolt shank (effective cross-section corresponding to the threaded part of the shank A_s=245 mm^2, for M20). Boundary conditions and loading procedures are the same as in the experiments. Particularly, each node of the back column flange has been constrained and a vertical load is applied on the transverse web stiffener of the beam. The finite element analysis procedure is based on incremental Newton-Raphson technique, while material and geometric nonlinearities are taken into account via the von Mises isotropic plasticity model and large displacement consideration.

The moment-rotation (M-φ) curves for the several connections are obtained from the beam vertical displacements and the applied load. The bending moment, M, acting on the connection corresponds to the applied load, L, multiplied by the distance, d, between the load application point and the face of the end-plate.

$$M = L \times d \tag{1}$$

The rotational deformation of the joint is the sum of the shear deformation of the column web panel zone and the connection rotational deformation. In these tests, the column hardly deforms as it behaves as a rigid element. Thus, the connection rotation φ is taken into account,

which is defined as the change in angle between the centerlines of beam and column and is approximately given by:

$$\varphi = arctan\frac{\delta}{d} - \theta_{b.el} \tag{2}$$

where δ: vertical displacement of the beam at the load application point, and $\theta_{b.el}$: beam elastic rotation (neglected in this study).

EC3-1-8 states that a bolted end-plate joint may be assumed to have sufficient rotation capacity for plastic analysis, provided that both conditions are satisfied: (i) the moment resistance of the joint is governed by the resistance of either the column flange in bending or the end-plate in bending; and (ii) the thickness, t, of either the column flange or the end-plate (not necessarily the same basic component as in (i)) satisfies:

$$t \leq 0.36\varphi_b\sqrt{\frac{f_{u.b}}{f_y}} \tag{3}$$

where φ_b: bolt diameter, $f_{u.b}$: tensile strength of the bolt, and f_y: yield strength of the relevant basic component. EC3-1-8 prediction for stiffness S_j is given by the relationship:

$$S_j = S_{j.ini}/\eta \tag{4}$$

where $S_{j.ini}$: initial stiffness evaluated according to the component method, and η: stiffness modification factor which in the context of an elastic-plastic global structural analysis is taken as 2.0 for bolted end-plate beam-to-column joints.

Moment-rotation (M-φ) curves of the above test specimens are presented next and compared with the experimental results by Coelho et al. [12] and Eurocode 3 suggestions [2]. Moreover, for each test, horizontal deformation of the end-plate is observed. The first three models are plotted in stress scale 0-35.5 kN/cm^2 and the last in 0-69.0 kN/cm^2 according to each end-plate yield stress. Four models are examined, one with shell elements and three with continuum elements. All of them predict accurately the elastic stiffness of the joints and generally are reliable in linear elastic static analysis. Bending of end-plates is the main reason for differences between these simulations in the elastoplastic region. For thin end-plates, which are dominated by bending (FS1, FS4), the use of continuum elements with reduced integration performs better. This simulation predicts almost exactly the three main joint behavioral characteristics, which are stiffness, resistance and rotation capacity. The normal brick element overestimates the elastic behavior of the joint, while the enhanced with incompatible modes gives more accurate results but remains stiff for this type of problems underestimating their high rotation capacity. Joint modeling with shell elements has a drawback. Bolt forces are applied locally to the nodes that connect the column flange with the end-plate and as a result there is local concentration of stresses, especially for very thin end-plates and/or column flanges. As the thickness of end-plate increases (FS2, FS3) the simulations tend to coincide. Brick elements with reduced integration remain the more flexible, while bricks with incompatible modes give also reliable results. Simulation with shell elements behaves very satisfactory and can be used for such type of problems.

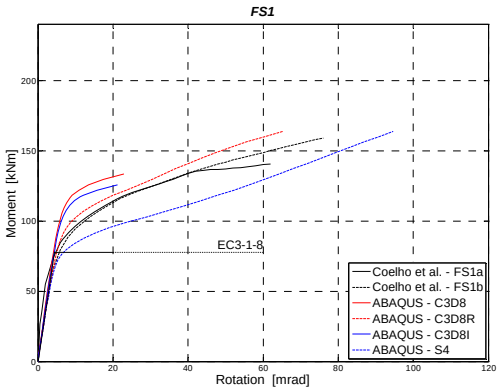

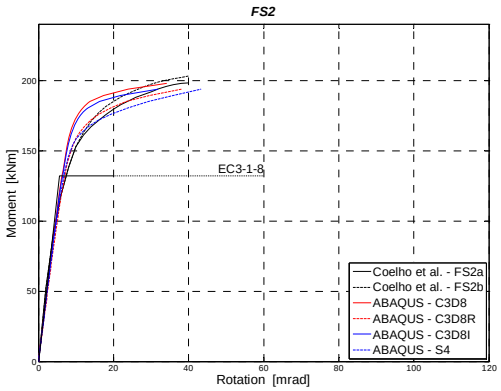

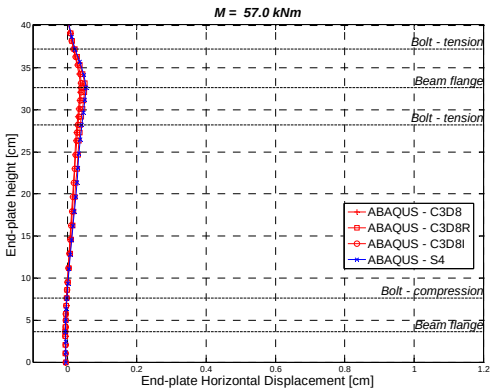

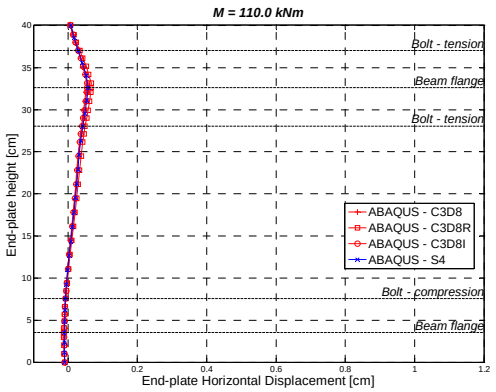

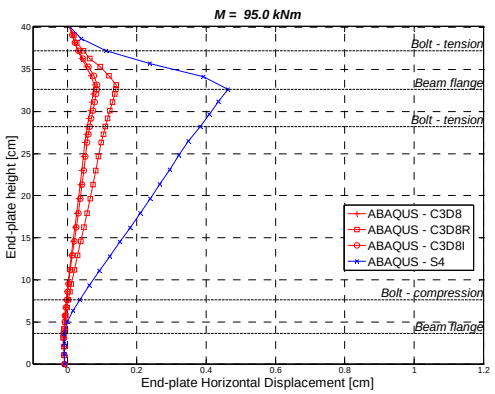

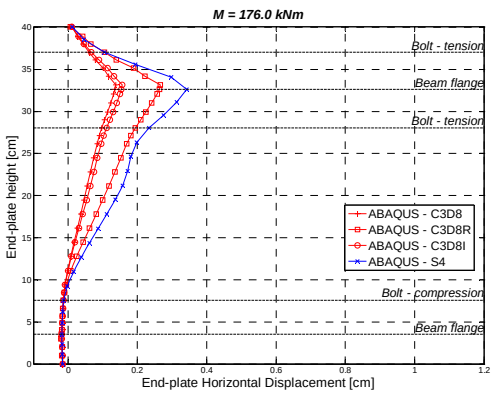

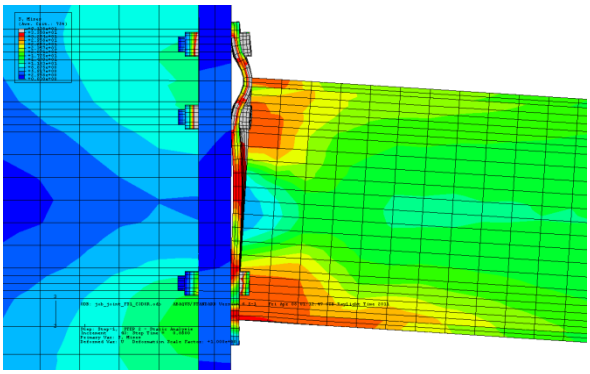

Figure 4: FS1 results

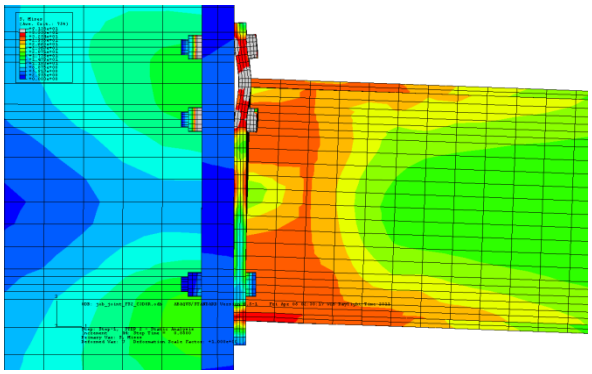

Figure 5: FS2 results

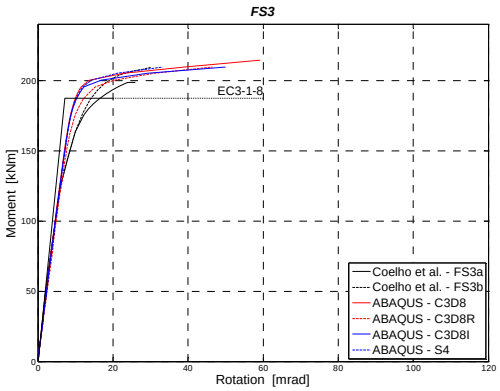

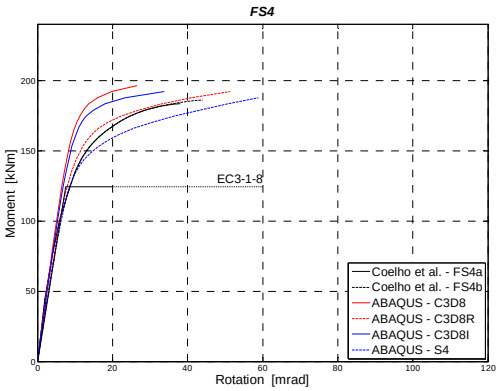

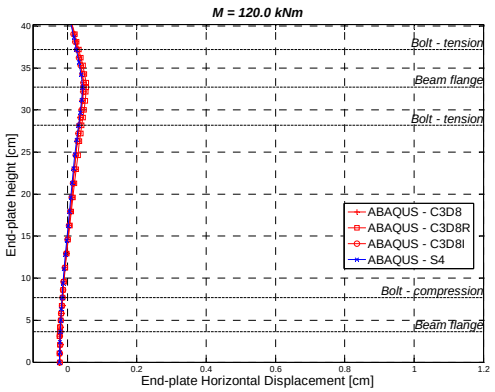

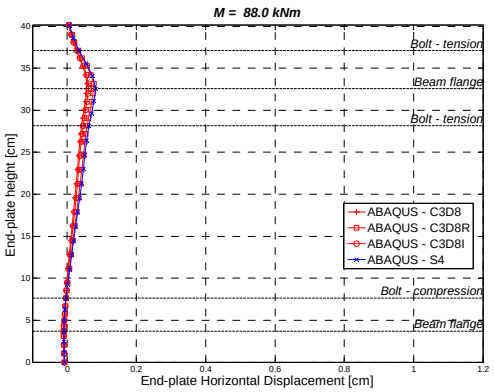

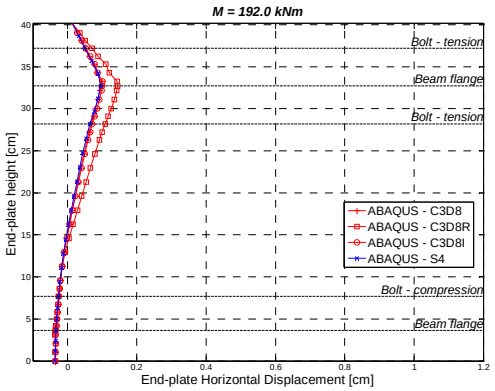

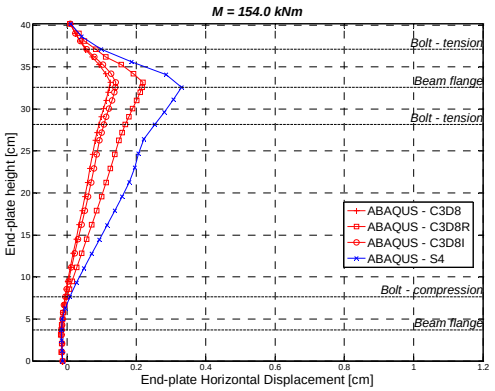

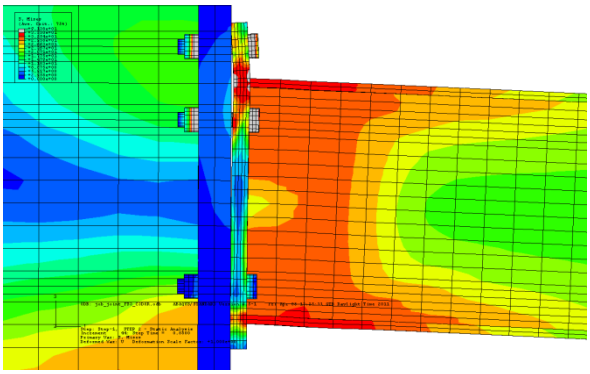

Figure 6: FS3 results

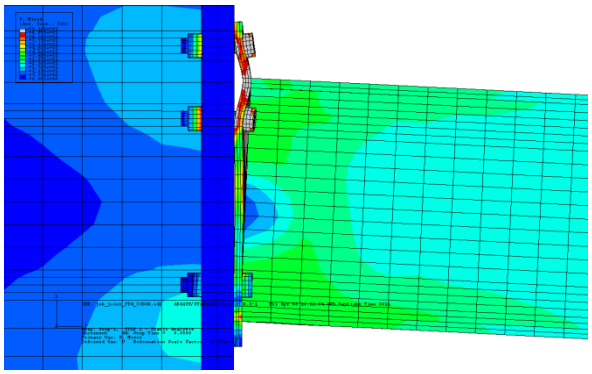

Figure 7: FS4 results

3 FINITE ELEMENT MODELING OF STEEL FRAMES

3.1 Numerical Modeling

Three different finite element simulations are examined: (i) *Type 1*: Simulation with beam elements for the members, while the joints are regarded as rigid; (ii) *Type 2*: Full simulation with shell elements for the members and detailed modeling of the joints according to 2.1 with shell and beam elements; and (iii) *Type 3*: Hybrid simulation with beam elements for the members and detailed modeling of the joints according to 2.1 with shell and beam elements. For this type of modeling proper compatibility constraints are assumed at the nodes of the interfaces. The length of the detailed joint part (beam/column) is taken as 0.10 of the corresponding total member length. The joints of this frame type are stiffened in two steps. In the first step (*Type 3 – stiff-a)*, transverse web stiffeners are added to the columns at the height of the beam flanges ($t_s = t_{fb}$), and in the second (*Type 3 – stiff-b*), apart from these stiffeners, supplementary web plates are added to the column webs ($t'_{wc} = 2t_{wc}$). It should be mentioned that the simulation with three-dimensional solid elements requires excessive computational time to perform an implicit direct-integration dynamic analysis that takes into account material and geometric nonlinearities including contacts. The simulation with structural elements is practically and computationally more efficient, even though there are some drawbacks in the modeling.

The hysteretic stress-strain model that has been adopted for the steel subjected to dynamic loading is displayed in Fig. 8. The steel grade specified for every component of each model, except for the bolts, is *S235* with the following characteristics: modulus of elasticity, E = 21000 kN/cm^2, yield stress, f_y = 23.5 kN/cm^2, ultimate stress, f_u = 36.0 kN/cm^2, and ultimate strain, ε_u = 0.25. The grade of bolts is 8.8 which means that $f_{y.b}$ = 64.0 kN/cm^2 and $f_{u.b}$ = 80.0 kN/cm^2, while their strain hardening modulus, E_t = 210 kN/cm^2.

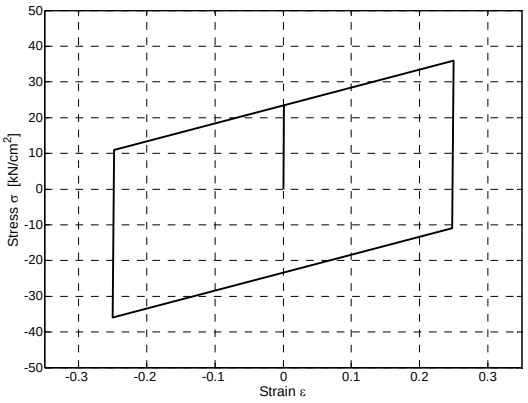

Figure 8: Hysteretic stress-strain (σ-ε) steel model

The general direct-integration method with the Hilber-Hughes-Taylor operator is used for the dynamic numerical analyses of this paper. It is an extension of the trapezoidal rule and is implicit, while a set of simultaneous nonlinear dynamic equilibrium equations must be solved at each time increment. The solution is done iteratively using Newton's method with material and geometric nonlinearities being included. A constant time step of 0.01 sec is used in the dynamic analyses.

Two kinds of damping are taken into account. The first is the artificial damping, through the numerical damping control parameter α. A value of α = -0.05 is used, which provides

slight numerical damping. The second is the material-Rayleigh damping, which introduces a damping matrix [C], defined as:

$$[\underline{C}] = \alpha_0[\underline{M}] + a_1[\underline{K}] \tag{5}$$

where [M]: the mass matrix, and [K]: the stiffness matrix of the model. Factors α_0 and α_1 can be derived from the solution of the following equations [4]:

$$\frac{1}{2}\begin{bmatrix} 1/\omega_i & \omega_i \\ 1/\omega_j & \omega_j \end{bmatrix}\begin{Bmatrix} \alpha_0 \\ \alpha_1 \end{Bmatrix} = \begin{Bmatrix} \zeta_i \\ \zeta_j \end{Bmatrix} \tag{6}$$

where $\omega_{i,j}$: natural frequencies of interest, and $\zeta_{i,j}$: damping coefficients for the corresponding natural frequencies of interest. For steel structures with bolted joints ζ can be taken conservatively as 6% = 0.06. In the analyses of this paper, only α_1 is used with α_1 = 0.0020 for the first frame test example and α_1 = 0.0025 for the second.

The frames are subjected to the 1940 Imperial Valley (El Centro) S00E horizontal component acceleration record. The 10 seconds acceleration history is shown in Fig. 9, while Fig. 10 depicts the response spectra for 2% and 6% damping. Peak ground acceleration (PGA) of 0.60g is chosen for the numerical analyses of the frames that follow.

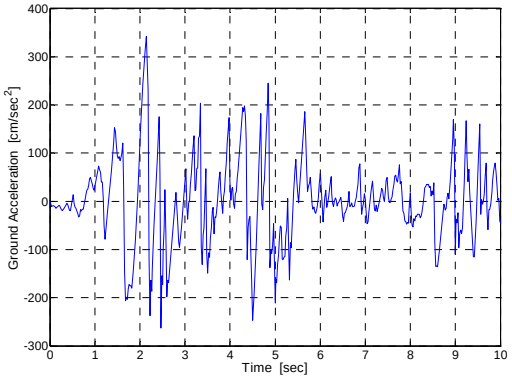

Figure 9: Acceleration time history of El Centro

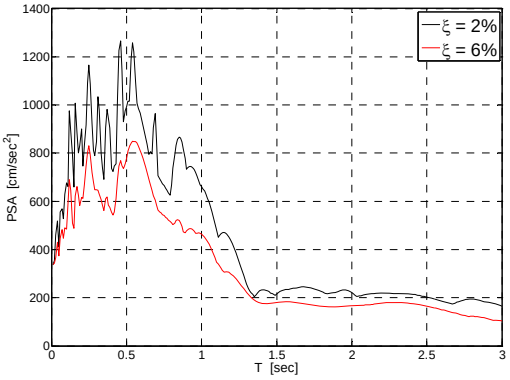

Figure 10: Response Spectra of El Centro

3.2 Frame No1

A steel frame of one opening (6 m) and two storeys (5 m each) is examined. Columns have a section profile HEB280 and beams IPE400. Details of the beam-to-column connections are shown in Fig. 11. Parametric studies on extended end-plate thickness, *t*, and bolts diameter, *D*, are performed. Each beam is assumed to have 20 times higher density than the density of steel (7850 kg/m^3) to account for the floor mass, while each column carries its own weight. The natural frequencies and periods are demonstrated in Table 2.

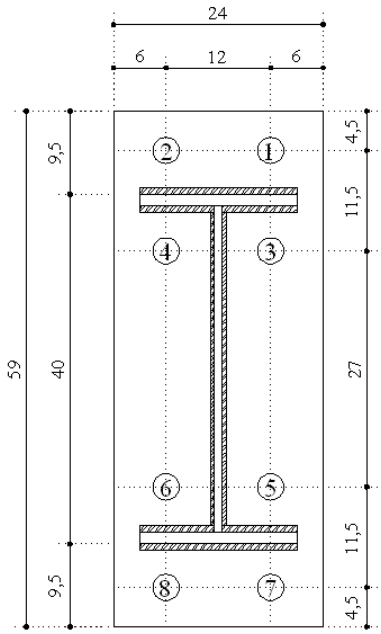

Figure 11: Bolted extended end-plate beam-to-column connection

Frame type	t (mm)	D (mm)	ω_1 (rad/s)	ω_2 (rad/s)	T_1 (sec)	T_2 (sec)
1	-	-	13.04	42.10	0.48	0.15
2	15	20	12.44	42.42	0.50	0.15
2	20	20	12.52	42.58	0.50	0.15
3	15	20	12.54	42.99	0.50	0.15
3	20	20	12.62	43.16	0.50	0.15

Table 2: Frame 1, Dynamic characteristics

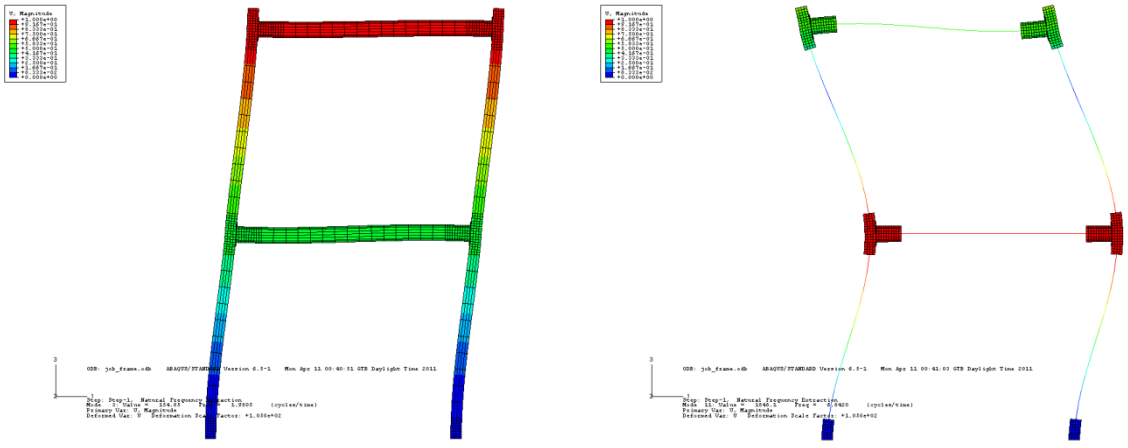

Figure 12: Frame 1, First and second mode

The results of various response analyses are presented in the next graphs. The parametric analyses (Figs. 13, 14) show that connection geometric characteristics do not affect the overall behavior of the frame with regard to the absolute maximum values. The tests performed showed that hybrid simulation is reliable and can be used instead of the full simulation, assuming that member beam elements do not exceed the yield stress, f_y, in order to account for the excessive computational effort required to perform nonlinear dynamic analyses with detailed finite element models. The comparisons between the different simulations are presented in Figs. 15-17.

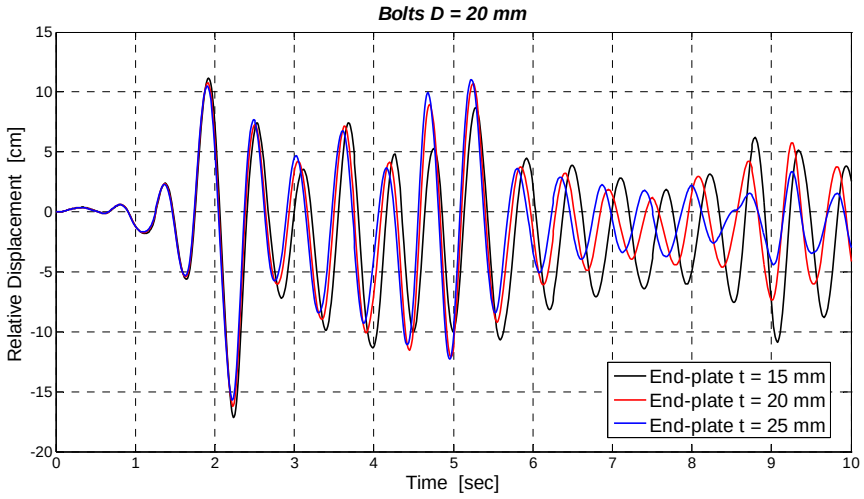

Figure 13: Frame 1, Simulation type 2, parametric analysis of end-plate thickness (2nd floor)

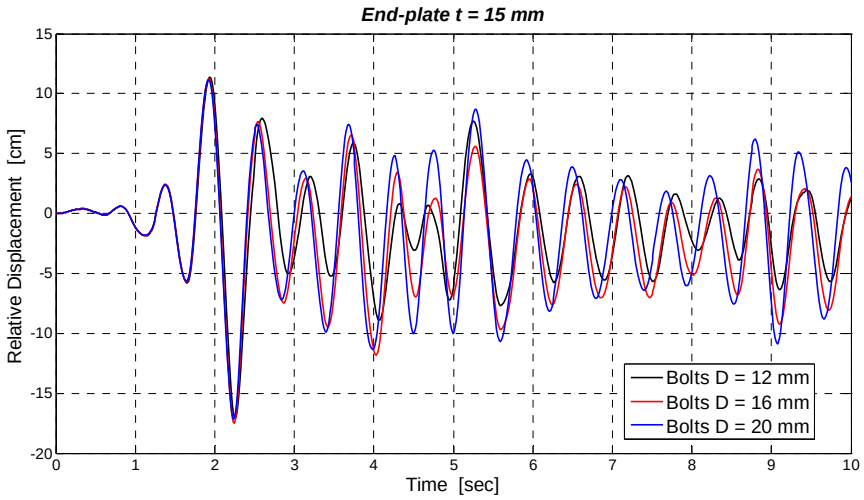

Figure 14: Frame 1, Simulation type 2, parametric analysis of bolts diameter (2nd floor)

Frame type	t (mm)	D (mm)	Iterations	Total CPU Time (sec)
1	-	-	1007	20
2	15	20	5018	8561
3	15	20	5002	5281
3 – stiff-a	15	20	4930	5688
3 – stiff-b	15	20	4593	5363

Table 3: Frame No1, CPU times

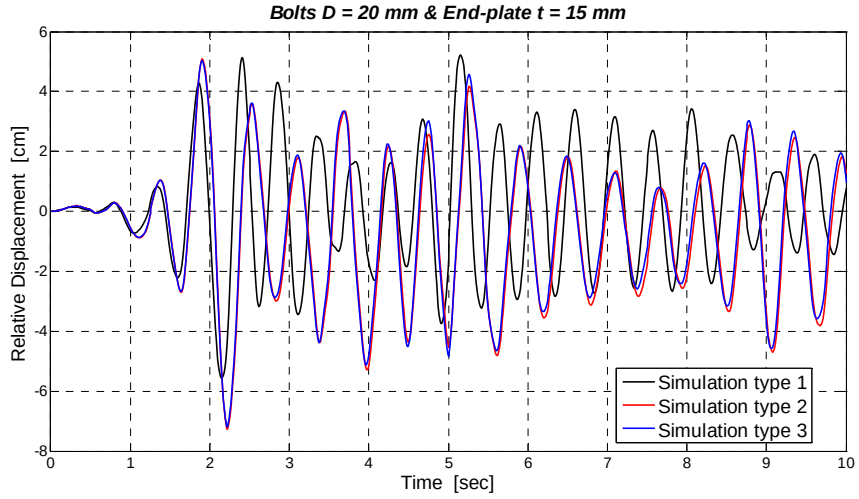

Figure 15: Frame 1, Comparison of simulation types (1st floor)

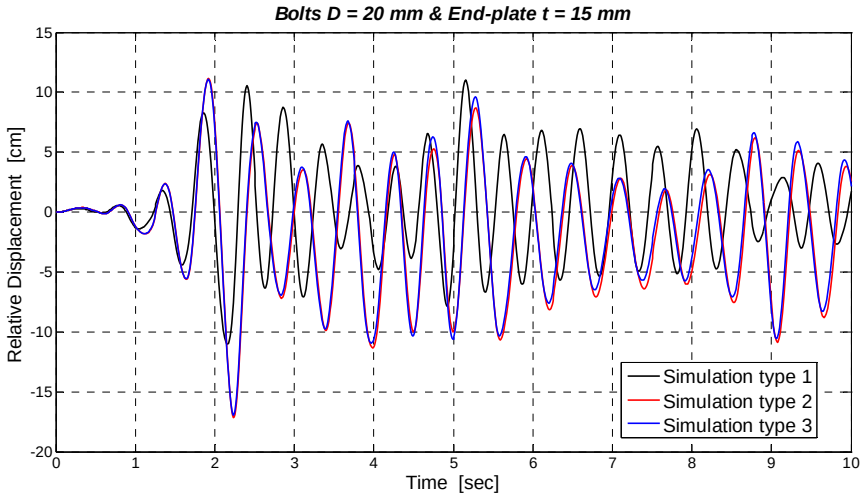

Figure 16: Frame 1, Comparison of simulation types (2nd floor)

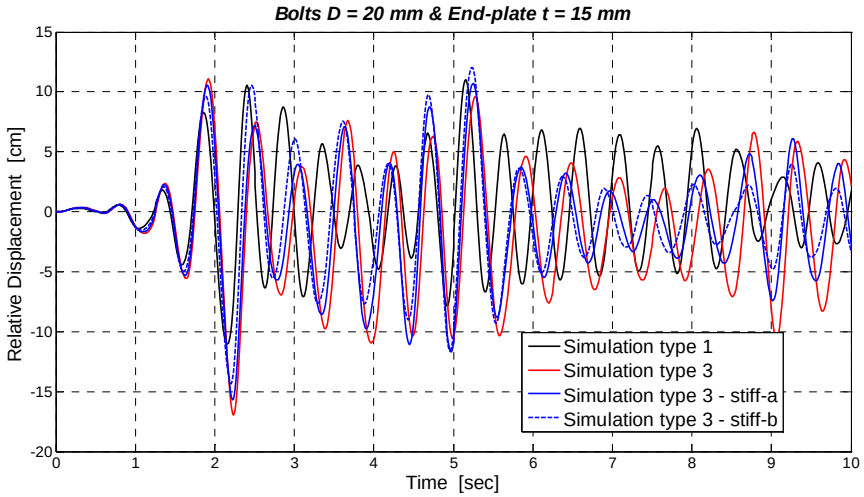

Figure 17: Frame 1, Influence of joint rigidity (2nd floor)

3.3 Frame No2

A steel frame of two openings (6 m each) and three storeys (4 m each) is examined. There are also double-sided joints apart from single-sided of Frame No1. Columns have a section profile HEB280 and beams IPE400. Beam-to-column connections are shown in Fig. 11. Each beam is assumed to have 20 times higher density than the density of steel (7850 kg/m^3) to account for the floor mass, while each column carries its own weight. The natural frequencies and periods are demonstrated in Table 4.

Frame type	t (mm)	D (mm)	ω_1 (rad/s)	ω_2 (rad/s)	T_1 (sec)	T_2 (sec)
1	-	-	10.66	34.25	0.59	0.18
2	15	20	10.00	33.51	0.63	0.19
2	20	20	10.10	33.79	0.62	0.19
3	15	20	10.10	34.01	0.62	0.18
3	20	20	10.20	34.29	0.62	0.18

Table 4: Frame 2, Dynamic characteristics

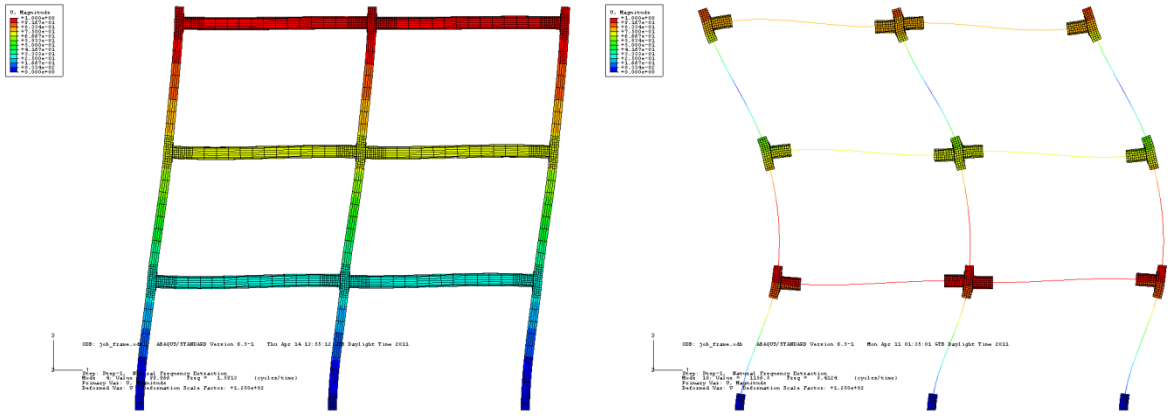

Figure 18: Frame 2, First and second mode

The results of the dynamic response of this test frame are presented in the next graphs. Parametric analyses (Figs. 19, 20) show that the geometric characteristics of the connections do not affect the overall behavior of the frame. As in the previous example, hybrid simulation is reliable and can be used instead of the full simulation, assuming that member beam elements do not exceed the yield stress, f_y. As the size of the problem increases, the computational effort required to perform nonlinear dynamic analysis with a detailed finite element model increases and the adoption of hybrid models becomes very useful and effective. For example, the time needed for a full simulation with shell elements of this frame is ~ 1.5 times greater than the time needed for a hybrid simulation. The comparisons between the different simulations are presented in Figs. 21-24.

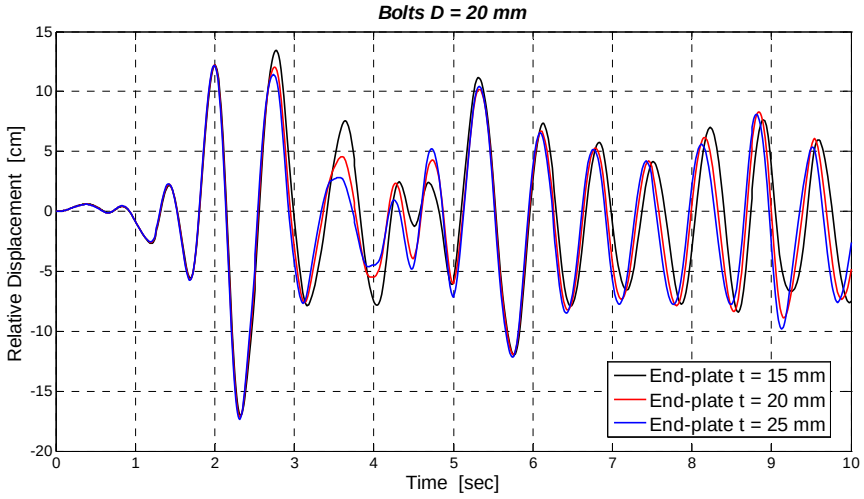

Figure 19: Frame 2, Simulation type 3, parametric analysis of end-plate thickness (3rd floor)

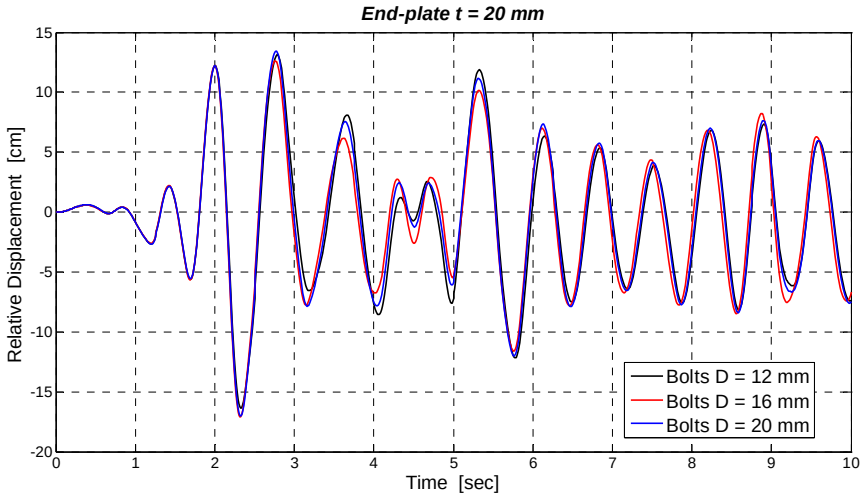

Figure 20: Frame 2, Simulation type 3, parametric analysis of bolts diameter (3rd floor)

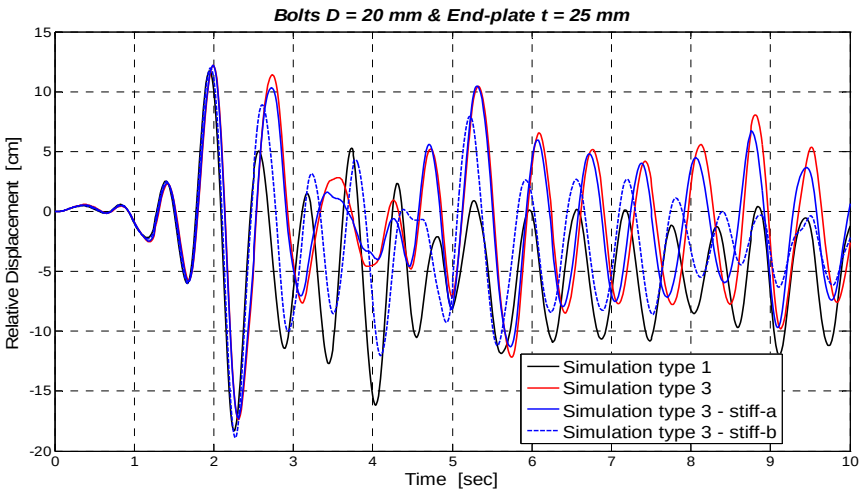

Figure 21: Frame 2, Influence of joint rigidity (3rd floor)

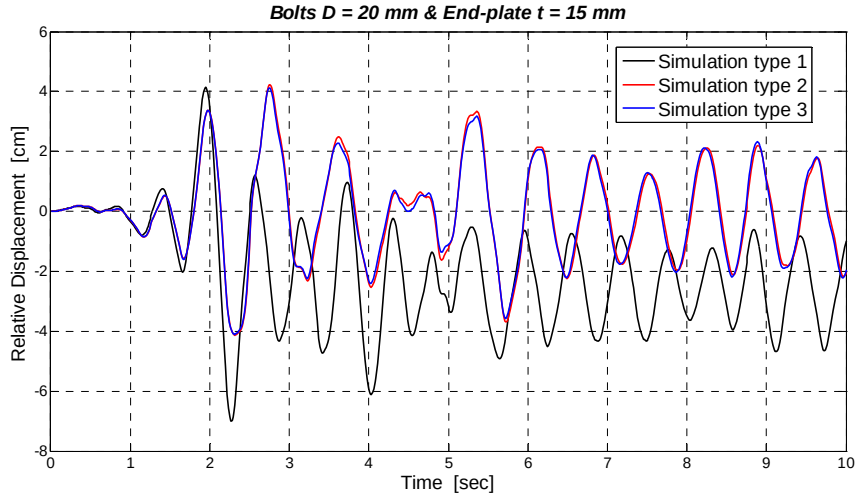

Figure 22: Frame 2, Comparison of simulation types (1st floor)

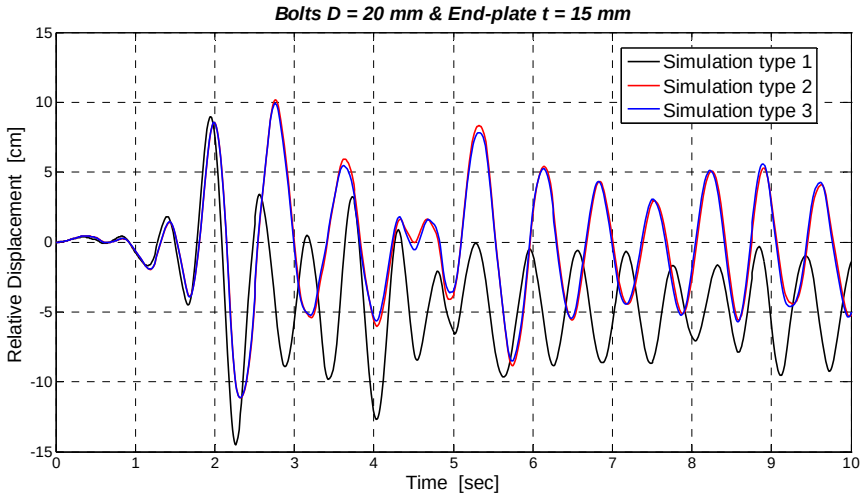

Figure 23: Frame 2, Comparison of simulation types (2nd floor)

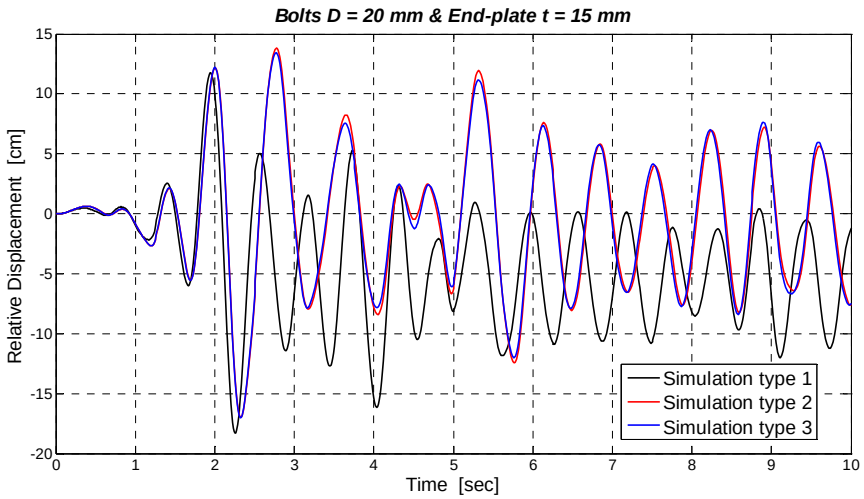

Figure 24: Frame 2, Comparison of simulation types (3rd floor)

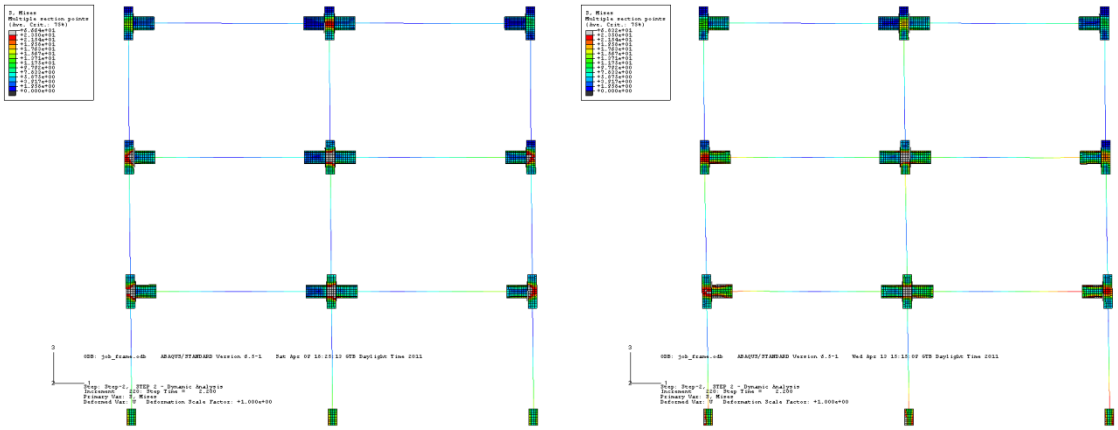

Figure 25: Frame 2, t=25mm, D=20mm, von Mises stresses distribution (t = 2.20 sec, *stress scale* 0: f_y), *Type 3* vs. *Type 3 – stiff-b*

Frame type	t (mm)	D (mm)	Iterations	Total CPU Time (sec)
1	-	-	1021	44
2	15	20	5401	22747
3	15	20	5368	15396
3	25	20	5694	17320
3 – stiff-a	25	20	5420	18232
3 – stiff-b	25	20	5390	18018

Table 5: Frame 2, CPU times

4 CONCLUSIONS

- Detailed finite element modeling considering material and geometric nonlinearities including appropriate contacts of bolted extended end-plate beam-to-column joints is performed, which can capture all local phenomena that affect the behavior of the joints under static or dynamic loads.
- Experimental results can be reproduced accurately using detailed joint models of hexahedral eight-node solid continuum finite elements with either reduced integration or incompatible modes depending on the plate thickness.
- Simulation with shell elements can be used for the modeling of steel joints with high level of accuracy in realistic problems, instead of continuum elements, which are computationally very demanding.
- Hybrid models, where the joints are modeled with shell elements and the connecting structural elements with beam elements, with appropriate kinematic constraints at the interfaces, give reliable results at reduced computational times.
- Modeling of frames with beam elements considering rigid joints fails to predict the semi-rigidity and the various types of failure of the joint structural components that may affect considerably the joint behavior.
- Parametric studies on extended end-plate thickness and bolts diameter of semi-rigid joints show that the connection geometric characteristics do not have a substantial effect on the seismic response of the overall structure.

REFERENCES

[1] ABAQUS version 6.5, *Analysis User's Manual*. 2004

[2] European Committee for Standardization (CEN), *EN 1993-1-8 – Eurocode 3: Design of Steel Structures –Part 1.8: Design of Joints.* 2005

[3] K.J. Bathe, *Finite Element Procedures*. Prentice-Hall, 1996

[4] Anil K. Chopra, *Dynamics of Structures, Theory and Applications to Earthquake Engineering, 3rd edition.* Pearson Prentice Hall, 2007

[5] M.R. Bahaari, A.N. Sherbourne, Computer modelling of an extended end-plate bolted connection. *Computers and Structures*, **52**(5), 879-893, 1994

[6] Mohammed R. Bahaari, Archibald N. Sherbourne, Behavior of eight-bolt large capacity endplate connections. *Computers and Structures*, **77**, 315-325, 2000

[7] O.S. Bursi, J.P. Jaspart, Calibration of a finite element model for isolated bolted end-plate steel connections. *Journal of Constructional Steel Research*, **44**(3), 225-262, 1997

[8] O.S. Bursi, J.P. Jaspart, Basic issues in the finite element simulation of extended end plate connections. *Computers and Structures*, **69**, 361-382, 1998

[9] Y.I. Maggi, R.M. Goncalves, R.T. Leon, R.F.L. Ribeiro, Parametric analysis of steel bolted end plate connections using finite element modeling. *Journal of Constructional Steel Research*, **61**, 689-708, 2005

[10] Anant R. Kukreti, Feng-Feng Zhou, Eight-bolt endplate connection and its influence on frame behavior. *Engineering Structures*, **28**, 1483-1493, 2006

[11] Charis J. Gantes, Minas E. Lemonis, Influence of equivalent bolt length in finite element modeling of T-stub steel connections. *Computers and Structures*, **81**, 595-604, 2003

[12] Ana M. Girao Coelho, Frans S. K. Bijlaard, Luis Simoes da Silva, Experimental assessment of the ductility of extended end plate connections. *Engineering Structures*, **26**, 1185-1206, 2004

[13] Ana M. Girao Coelho, Frans S.K. Bijlaard, Experimental behaviour of high strength steel end-plate connections. *Journal of Constructional Steel Research*, **63**, 1228-1240, 2007

[14] L.R.O. de Lima, L. Simoes da Silva, P.C.G. da S. Vellasco, S.A.L. de Andrade, Experimental evaluation of extended endplate beam-to-column joints subjected to bending and axial force. *Engineering Structures*, **26**, 1333-1347, 2004

[15] Yongjiu Shi, Gang Shi, Yuanqing Wang, Experimental and theoretical analysis of the moment-rotation behaviour of stiffened extended end-plate connections. *Journal of Constructional Steel Research*, **63**, 1279-1293, 2007

[16] A.S. Elnashai & A.Y. Elghazouli, Seismic Behaviour of Semi-rigid Steel Frames. *Journal of Constructional Steel Research*, **29**, 149-174, 1994

[17] Gang Shi, Yongjiu Shi, Yuanqing Wang, Behaviour of end-plate moment connections under earthquake loading. *Engineering Structures*, **29**, 703-716, 2007

[18] Minas E. Lemonis, Charis J. Gantes, Mechanical modeling of the nonlinear response of beam-to-column joints. *Journal of Constructional Steel Research*, **65**, 879-890, 2009